

## Diagnostics of zinc selenite plasma produced by FHG of a Q-switched ND: YAG laser

N. Kh. Abdaalameer, S. N. Mazhir, K. A. Aadim

<sup>a</sup>University of Baghdad, College of Science for woman, Iraq

<sup>b</sup>University of Baghdad, College of Science, Iraq

We presented the OES studies of the Zinc Selenite ZnSe plasma produced by the FHG (1064nm) of a Q-switched ND: YAG laser. The target material was placed in front of laser beam in air at atmospheric pressure. The experimentally observed line profiles of zinc (ZnI) have been used to extract the Te using the Boltzmann plot method. Whereas, the ne has been determined from the Stark broadening method using the Zinc (Zn I) line. And it is calculated  $\omega_p$ ,  $\lambda_d$  and  $N_d$ . The Te is calculated by varying the laser energy at (100, 200, 300, 400 and 500) mJ. It is observed that  $T_e$ ,  $n_e$  and  $\omega_p$  increases as laser energy is increased while  $\lambda_d$  and  $N_d$  decreases as laser energy increased.

(Received March, 21, 2021; Accepted July 12, 2021))

*Keywords:* OES, ZnSe, FHG,  $T_e$ ,  $n_e$ ,  $\omega_p$ ,  $\lambda_d$ ,  $N_d$

### 1. Introduction

Laser mediated breakdown spectroscopy is a powerful simple research tool for a number of product applications in the form of solids, liquids and gases, such as material analysis, environmental monitoring[1]. Effectively absorbed by isothermally expanding plasma. In the third stage, the plasma pruning resulting spreads quasi-adiabatically in a medium after the end of the laser pulse, which may include vacuum or background gas with or without fields applied[2]. Sample types can vary widely Since optical processes of absorption trigger the LIBS sampling so that solids, liquids and gasses can be analyzed[3]. The plasma is created If the energy from the laser pulses heats, the sample material is ablated, atomized and ionized. A spectrograph and a detector then spectrally resolve and detect the plasma plume. The resulting plasma spectrum can deduce information's both quantitative and qualitative, as in the elementary composition. Details of plasma temperature and electron density can be given by emitting line properties, such as widths, shapes and changes [4]. Because of its ability to define and model such plasma properties, such as relative energy level populations and particle velocity distribution, plasma temperature is a significant thermodynamic property. The present laboratory experiment has used the two-line hydrogen ratio method that implies that the local plasma thermodynamic equilibrium (LTE) is preserved. The ratio approach is a popular means of measuring plasma temperature, and it is possible to calculate the strength ratio of a pair of atomic spectral lines or ions at the same degree of ionization [5]. The material under this study of ZnSe both the elements separately as well as in the form of either compound remained under research since long due to their various uses / application in various fields[6].

This also relies on observing the shape and width of spectral lines which several mechanisms can change. The plasma electron temperature can be measured using Boltzmann plot. The Boltzmann plot method is a simple and commonly used method for spectroscopic measurement, especially for measuring plasma electron temperature from the relative intensity of a spectrum of two or more lines having a relatively large energy difference. Nevertheless, in order to use the Boltzmann plot method to calculate electron temperature in practice, the excitation point must be reached under an LTE condition. The latter helps us to use traditional plot technique from Boltzmann to evaluate T using the expression[7]:

$$\ln \left[ \frac{\lambda_{ji} I_{ji}}{c A_{ji} g_{ji}} \right] = -\frac{1}{KT} (E_j) + \ln \left[ \frac{N}{U(T)} \right] \quad (1)$$

\* Corresponding authors: nesreen.khaleel1004a@csu.uobaghdad.edu.iq  
<https://doi.org/10.15251/CL.2021.187.405>

where  $I_{ji}$  is the relative intensity (in arbitrary units) of the emission lines between the energy levels  $i$  and  $j$ , its wavelength (in nanometres),  $g_{ji}$  is the degeneration or statistical weight of the emitting upper level  $i$  of the transition measured, and  $A_{ji}$  is the transition probability of spontaneous radiative emission from the level  $i$  to the lower level  $j$ . Eventually,  $E_j$  is the level  $i$  (in eV) excitation energy,  $k$  is the Boltzmann constant, densities of the  $N$  state population. The Stark broadening is due to the displacement of the two layers of a heavy particle (ion or atom) in a radiative transition during its interaction with a charged particle[8]. It thus relies on both the atomic structure and its surrounding. Since "the line-broadening device" shows a Lorentzian form, the Stark profiles of plasma atomic lines are formed by ion low-frequency fields and by high-frequency electron fields[9]. The width of the stark line ( $\Delta\lambda_{FWHM}$ ) can be determined by extracting the instrumental line broadening ( $\Delta\lambda_{instrument}$ ) from the line width ( $\Delta\lambda_{observed}$ ) as below:

$$\Delta\lambda_{FWHM} = \Delta\lambda_{observed} - \Delta\lambda_{instrument} \quad (2)$$

where  $\Delta\lambda$  is the "real" FWHM, and where the parameter ( $n_e, T_e$ ) specifies the relative contribution of electron collision to electrostatic fields, it is weakly dependent on  $n_e$  and  $T_e$ , which can normally be regarded as constant. The electrical field that produces a Stark effect in laser-plasma is mainly the product of collisions with electrons, with minor contributions due to collisions with ions. So the eq. can be simplified[10]:

$$n_e = \left[ \frac{\Delta\lambda}{2\omega_s} \right] N_r \quad (3)$$

$\omega_s$  is the theoretical line full width Stark broadening parameter, calculated at the same reference electron density  $N_r \approx 1.1 \times 10^{18} \text{ cm}^{-3}$ , [11]. We can define a Debye sphere as a sphere inside the plasma of radius equal to  $\lambda_D$ . The Debye length ( $\lambda_D$ ) is directly proportional to the square root of the temperature ( $T$ ) and inversely proportional to the square root of the electron number density ( $n_e$ ) according to [12]:

$$\lambda_D = \left( \frac{\epsilon_0 k T}{n_e e^2} \right)^{1/2} \quad (4)$$

where  $\epsilon_0$  is the permittivity of free space,  $k_B$  the Boltzmann constant and  $e$  the electron charge. It can be showed that the Debye length is a function of the electron and ion temperatures,  $T_e$  and  $T_i$ , and the plasma density  $n_e \cong n_i$  (assuming singly charged ions). When the electrons move under force of electric field from the charge balance, they response to the field, and accelerate then they tend to overshoot and execute an oscillatory motion. These oscillations occur at frequency called Plasma frequency of electron ( $\omega_{pe}$ ) which can be written as [13]:

$$\omega_{pe} = \sqrt{\frac{e^2 n_e}{\epsilon_0 m_e}} \quad (5)$$

And in frequency unite,  $\omega_{pe}$  given approximately by:

$$\omega_{pe} = \frac{\omega_{pe}}{2\pi} \approx 8.98 \sqrt{n_e} \text{ (Hz)} \quad (6)$$

where  $\omega_{pe}$  is the plasma frequency of electron [13]. In the end, results were analyzed and compared with (NIST) [14].

In this paper, ZnSe plasma is described in terms of zinc selenite fraction and operating parameters utilising OES to investigate the production of active species. The electron temperature, which also influences the plasma reactivity through inelastic collisions producing the active species, is evaluated from ZnI and SeI spectral line intensities using the Boltzmann plot method.

The key aims of this paper are to underpin the plasma reactivity species and to achieve a better understanding of the mechanisms regulating the development of these species.

## 2. Experimental part

### 2.1. Laser system

Laser Nd: YAG (HuaFei Tong Da teq. Diamond – EPLS 288 Pattern) with various peak power was used in the plasma creation process under Vacuum. The key technological parameters are:

- Laser design: Q- First harmonic generation of Nd: YAG Laser switched
- Power peak laser: (6-3) mW.
- Wavelength laser: (1064)nm.
- Frequency of repeating: (1-6) Hz.
- Process of cooling: inner circulation water cooling.
- Power supply data Ac: (220) Volt.

### 2.2. Experimental work

It is shown that by increasing the distance between laser lens and target can change the spot laser diameter. The duration of pulse is (9 ns) with frequency 6 Hz, and a wavelength of 1064 nm, which is he precise distance to machine accuracy and precision during the measurements.

The focal length of the lens is 10 cm. A shorter focal lens can be used to establish a small beam size and thus a better breakdown, but it also has a smaller focal depth, Fig. 1 shows the LIBS Configuration Schematic Diagram.

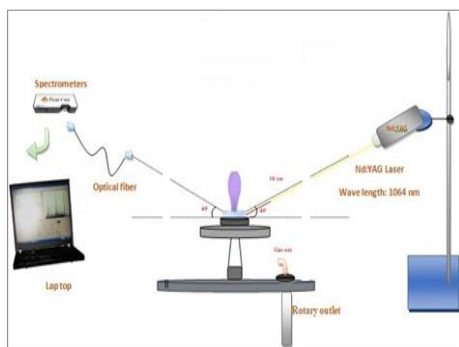


Fig.1. Device design for the laser-induced plasma spectroscopy (LIBS).

The spectrometer study was conducted by using the light produced by the pulsed laser from a sample bombarded. The fast response time spectrometer (HR 4000 CG-UV-NIR) of Ocean Optics is used to measure the light emitted during setup.

The optical fibers, in an angle of approximately 45 degrees to the laser beam axis to avoid splash, absorbed the light emitted by the flushed plasma, and was then guided into the spectrometer slit entrance. Depending on the gate used in the spectrometer, laser Nd: YAG was closely focused on plasma pen production; and with its wavelength of 3648 pixels, it responded with a wavelength of 300-700 nm. The spectrum of plasma was of different value of energies, and this was done by preparing 2 g of zinc, 2 g of selenium, and mixing them at percentage (X=0.5), and the pulse laser energy was varied from 100 to 500 mJ. Each spectrum was obtained within wavelengths of (300-700) nm.

Finally, the data are analyzed and measured via the National Institute of Technology and Standards (NIST) [15]. Besides, parameters of plasma, such as ( $n_e$ ), ( $T_e$ ) are measured and the characteristics of the plasma are determined.

### 3. Result and discussion

#### 3.1. Evaluation of plasma parameters for (ZnSe) target

The optical emission spectrum of laser-produced Zinc selenite plasma in air ranging from 300 nm to 700 nm is shown in Fig. 2, with E=(100, 200, 300, 400, 500) mJ, this figure clearly shows the strength of the changes in spectral lines with the rise in laser peak power. This can be described as follows: Increased laser energy increases the target's total ablation rate, which means increasing the excited atoms and thus increasing the spectral intensity.

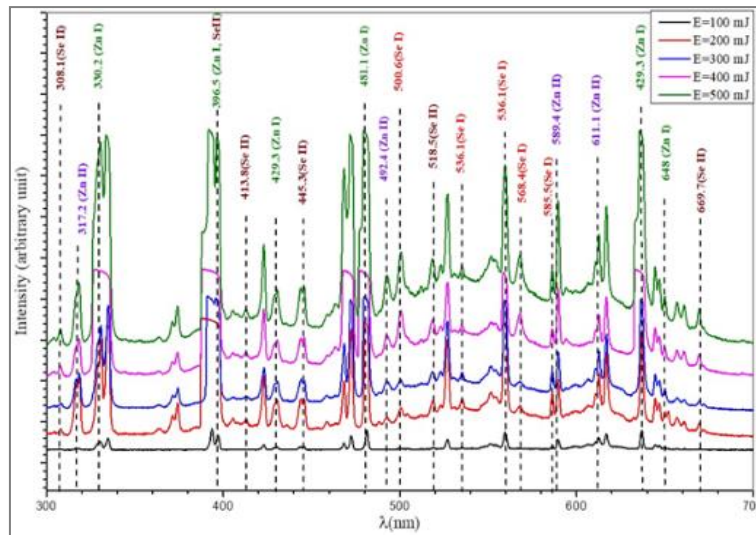


Fig. 2. Emission spectra of laser induced on Zinc Selenide target with different laser energies (100, 200, 300, 400 and 500).

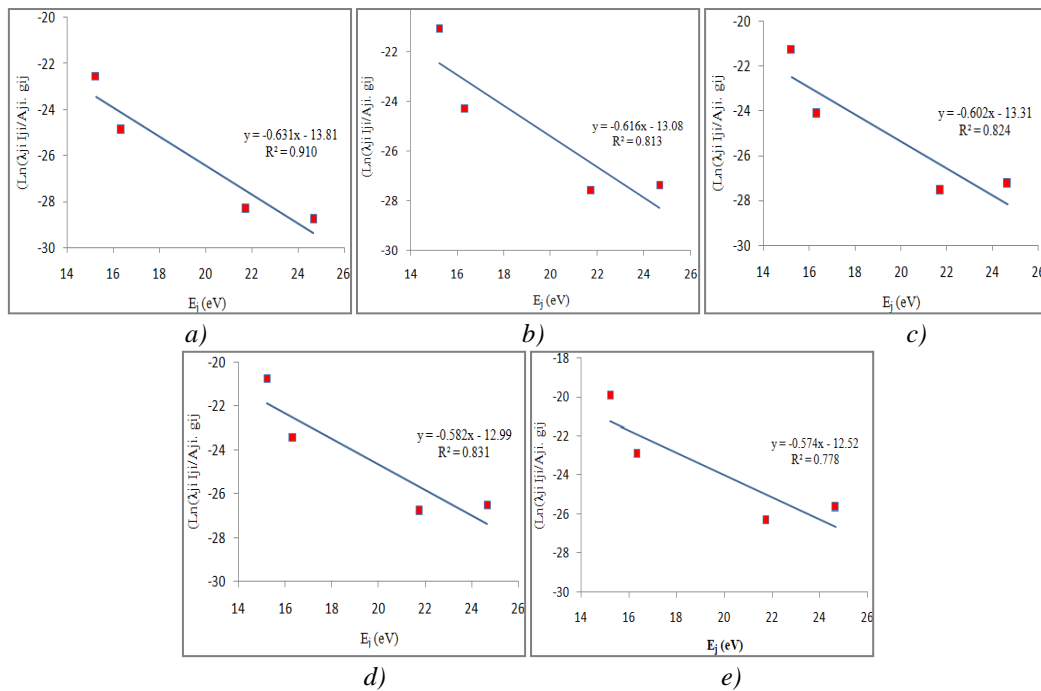


Fig. 3. Boltzmann plot of plasma emission for (ZnSe) target at different laser energy. a) 100 mJ; b) 200mJ; c) 300mJ; d) 400 mJ; e) 500 mJ

The Boltzmann plot restricted the electron temperatures ( $T_e$ ) of the best linear fit slope. Boltzmann's plot includes a war of the same atomic form and the process of ionization itself (select five peaks for ZnI at 308.624 nm, 445.588nm, 518.552nm and 669.94nm), as shown in Fig.3.

The electron densities were determined using stark broadening from Eq.(3). In Fig. 4. High extension of the plasma spectral lines results from a collision with the charged particles, which expands the line and the peak wavelength change.

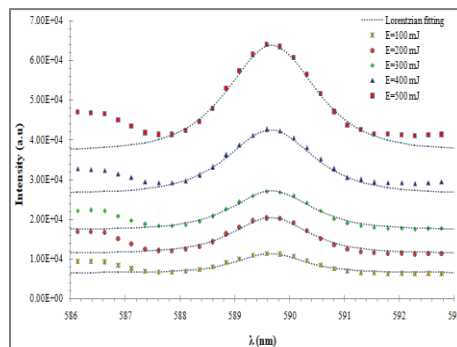


Fig.4. Stark broadening for 589.65nm ZnII line.

### 3.2. Determination of temperature and density of the electron

Fig. 5 displays the Laser Power Density difference of  $T_e$  and  $n_e$ . The results of these statistics showed that the rise in laser power density has resulted in an increase in electron temperature and electron density due to the plasma absorption of the laser photon. The rise in  $n_e$  contributed to the rise in electron collisions with the increase in laser power density.

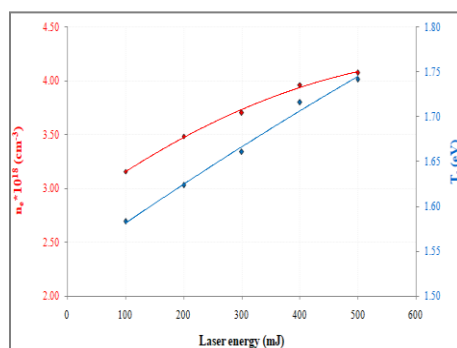


Fig. 5. Clarification of  $T_e$  and  $n_e$  versus the laser energy.

Obviously, Fig. (5) shows the magnitude of the spectral lines is increasing with the rise in the peak strength of the laser, which can be identified as interpreted:

The rise in laser intensity causes the rate of mass ablation from the target to increase, This indicates more excited atoms and hence an improvement in the intensity of the spectral line height. Increased laser power can boost plasma absorption, leading to greater ablation. This is why, with plasma emissions, laser peak power grows linearly.

In the two separate lines, the prominent component target of zinc selenide (ZnSe) is observed in spectral lines and the plasma parameters are calculated using these data.

Temperature ( $T_e$ ) of electrons and density of electrons ( $n_e$ ) measurement values using the Saha-Boltzmann equation (Eq.2) show that as the laser pulse energy increases in air, temperature of electron and density of electron increases as shown in figure (5), this agrees with the findings stated in a previous study[16].

Fig. (6.a,b) indicates that while the plasma frequency increases ( $f_p$ ), the Debye duration ( $\lambda_D$ ) decreases, with the laser pulse intensity rising because of its proportional to ( $n_e$ ) for the zinc selenide part. This corresponds with the findings stated in a previous study [17].

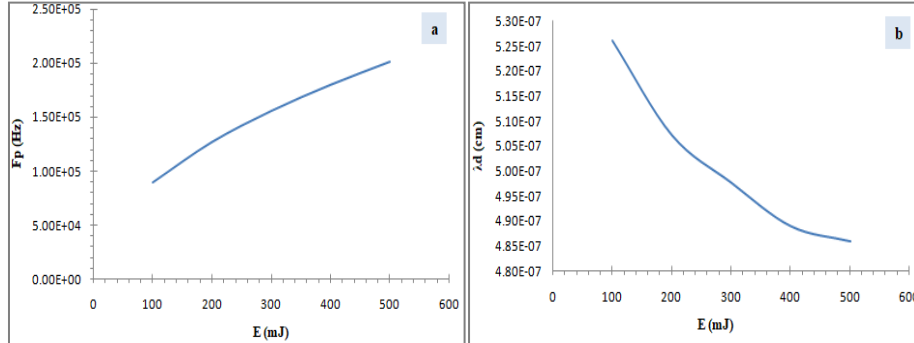


Fig.6.Show that the laser energy as a function of (a) ( $f_p$ ), (b)( $\lambda_d$ ), for Zinc Selenite.

The measured electron temperature ( $T_e$ ), electron density ( $n_e$ ), Debye length ( $\lambda_D$ ), plasma frequency ( $f_p$ ), Debye number ( $N_d$ ) for the ZnSe target at various laser energies are shown in Table (1). All parameters measured in the plasma sample ( $\lambda_d$ ,  $f_p$ , and  $N_d$ ) have fulfilled the requirements for going on with the plasma.

Table 3.ZnSe plasma parameters of varying laser energies.

E (mJ)	FWHM (nm)	$T_e$ (eV)	$n_e$ ( $\text{cm}^{-3}$ )	$f_p$ (Hz)	$\lambda_D$ (cm)	$N_d$
100	1.45	1.583132	3.16E+18	1.59585E+13	5.26055E-07	1.925816
200	1.6	1.623311	3.48E+18	1.67636E+13	5.07105E-07	1.903556
300	1.7	1.660447	3.7E+18	1.72796E+13	4.97559E-07	1.910451
400	1.82	1.715842	3.96E+18	1.7879E+13	4.88832E-07	1.939561
500	1.87	1.741177	4.07E+18	1.8123E+13	4.858E-07	1.95599

#### 4. Conclusions

It was found that intensity increases at various laser peaks with When strength begins to rise, laser peak intensity then declines. The intensities of laser-induced plasma emission spectrum lines have been found to be highly dependent on the environmental conditions. Laser beam contact with metal targets is a very effective way of making plasma columns composed of highly concentrated electrons, ions, and neutral molecules. Laser-induced plasma spectra were found to show strong spectral lines for the air environment and increase their strength, thus increasing Pulse Laser Energy. The results showed that laser energy was lowered at values ( $N_d$ ,  $\lambda_d$ ) and the value ( $f_p$ ,  $n_e$ ,  $T_e$ ) was increased in laser power for ZnSe. Parameters of plasma including (density of electron and temperature of electron, number of particles in the sphere Debye, plasma frequency, and Debye length) strongly affect laser energy.

## Acknowledgements

The team work would like to thank Plasma Physics Lab in the Department of Physics at the University of Baghdad, College of Science for helping to promote and sustain this work.

## References

- [1] N. M. Shaikh, M. A. R. Nizamani, A. H. Moghal, Sindh Univ. Res. J. **45**(2), 399 (2013).
- [2] N. M. Shaikh, Y. Tao, R. A. Burdt, S. Yuspeh, N. Amin, M. S. Tillack, J. Phys. Conf. Ser. **244**(4), 2 (2010).
- [3] M. L. Najarian, R. C. Chinni, J. Chem. Educ. **90**(2), 244 (2013).
- [4] David A. Cremers, Handbook of Laser-Induced Breakdown Spectroscopy, 2nd Editio. USA, 2013.
- [5] N. K. Abdulameer, Impact of Dielectric Barrier Discharge ( DBD ) Plasma on the Optical Properties of Thin Films, **15**(8), 1937(2020).
- [6] N. Kh. Abdulameer, S. N. Mazhir, K. A. Adim, Energy Reports **6**(6), 447 (2020).
- [7] H.-H. Ley, Journal of Science and Technology **6**(1), 1 (2014).
- [8] C. Aragón, J.A. Aguilera, Spectrochimica Acta Part B: Atomic Spectroscopy **63**(9), 893 (2008)
- [9] N. Yang, Masters Theses, 89 (2009).
- [10] X. Bai, Laser-induced plasma as a function of the laser parameters and the ambient gas, 2014.
- [11] N. W. Konjević, Journal of physical and chemical reference data **19**(6), 1307 (1990).
- [12] F. Anabitarte, A. Cobo, J.M. Lopez-Higuera, Laser-induced breakdown spectroscopy: fundamentals, applications, and challenges. ISRN Spectroscopy, 2012.
- [13] M. Cvejić, Journal of Physics: Conference Series, 2014.
- [14] National Institute of Standards and Technology (NIST) Atomic spectra database, Version 5, 2017.
- [15] J. Y. Pae, R. Medwal, J. Vimal, M. V. Matham, R. S. Rawat, J. Vac. Sci. Technol. B **37**, 041201 (2019).
- [16] S. N. Mazhir, K. A. Adim, N. Abdulameer, A. H. Ali, IOP Conf. Ser.: Mater. Sci. Eng. **987**, 012020 (2020).
- [17] M. A. Essa, A. A. Kadhim, Iraqi Journal of Physics **17**(42), 125 (2019).